



ARTICLE

3D Printed PEDOT:PSS Flexible Electrochromic Devices for Patterned Displays

Manting Song^{1,2}, Changchen Gong^{1,3} and Ximei Liu^{1,2,*}

¹Jiangxi Provincial Key Laboratory of Flexible Electronics, Jiangxi Science and Technology Normal University, Nanchang, 330013, China

²School of Pharmacy, Jiangxi Science and Technology Normal University, Nanchang, 330013, China

³College of Chemistry and Chemical Engineering, Jiangxi Science and Technology Normal University, Nanchang, 330013, China

*Corresponding Author: Ximei Liu. Email: liuxm@jxstnu.edu.cn

Received: 01 September 2024 Accepted: 27 November 2024 Published: 27 March 2025

ABSTRACT

Flexible electrochromic devices (FECDs) demonstrate significant potential for applications in wearable electronics, military camouflage, and flexible smart displays. As a crucial electrochromic material, poly(3,4-ethylenedioxythiophene):polystyrene sulfonate (PEDOT:PSS) is widely used in FECDs due to its excellent mechanical flexibility, tunable conductivity, and non-toxicity. However, the manufacturing process for patterned PEDOT:PSS electrochromic devices remains intricate, costly, and challenging to personalize. To address this challenge, we have developed a 3D-printable ink with controllable rheological properties through a concentration-tuning strategy, enabling programmable, patterned printing of PEDOT-based conductive polymer electrochromic layers. The 3D-printed FECDs exhibit outstanding electrochromic performance, including a high optical contrast (up to 47.9% at 635 nm), fast response times ($t_c = 1.6$ s; $t_b = 0.6$ s), high coloration efficiency ($352 \text{ cm}^2 \text{ C}^{-1}$), and good cycling stability (with only a 9.3% decrease in optical contrast after 100 electrochemical cycles). Finally, we utilize 3D printing technology to construct flexible, patterned PEDOT:PSS electrochromic devices with bespoke butterfly designs. This work establishes the theoretical foundation for the application of 3D printing technology in PEDOT:PSS flexible electrochromic devices.

KEYWORDS

3D printing; PEDOT:PSS; flexible electrochromic device; patterned displays

1 Introduction

In recent years, technological advancements and the drive for smarter living have propelled the development of wearable electronics such as robotic skins and optoelectronic devices [1–3]. Electrochromic devices (ECDs) hold significant potential due to their low power consumption, fast response times, and excellent controllability, making them well-suited for applications in smart displays [4], wearable devices [5], and smart windows [6]. Electrochromism refers to the phenomenon where a



material's optical properties, such as absorbance and transmittance, change under an external electric field, resulting in a reversible color change [7].

Electrochromic materials can be categorized into inorganic and organic categories [8–10]. Inorganic electrochromic materials, predominantly based on transition metal oxides and their derivatives, such as cathodic coloring from Group VI B metal oxides [11–13] and anodic coloring from Group VIII B metal oxides [14,15], are renowned for their rapid response and exceptional stability. These materials are capable of fast color change and maintaining stability over prolonged periods [16–18]. However, despite these advantages, the production costs of inorganic electrochromic materials remain relatively high. In contrast, organic electrochromic materials offer advantages such as a broad spectrum of colors, ease of processing, low production costs, and highly tunable molecular structures [19–21]. Conductive polymers [22,23], in particular, exhibit reversible color changes during the doping and dedoping process, alongside benefits such as low driving voltage, vibrant color transitions, short response times, high optical contrast, affordability, ease of molecular customization, and excellent processability. PEDOT:PSS has been extensively studied due to its superior water dispersibility [24–26], controllable miscibility, and adjustable conductivity. Because of these advantages, PEDOT:PSS has found widespread applications in bioelectronics [27–29], flexible wearables, and other fields. Notably, Naoji Matsuhisa and Professor Zhenan Bao's team at Stanford University have utilized PEDOT:PSS as a functional material for pixel integration, enabling visual signal representation in strain sensors [30]. Although PEDOT:PSS hydrogels have been incorporated into electrochromic devices [5], the use of PEDOT:PSS in dry-film electrochromic devices has not yet been explored.

However, the fabrication of flexible PEDOT:PSS electrochromic devices still faces challenges, such as complex manufacturing processes, high costs, and difficulties with personalization, which significantly limit their potential for low-cost, large-area patterned production [31–33]. To address these challenges, there is an urgent need to develop a low-cost, efficient, and programmable fabrication technique [34,35]. As an innovative additive manufacturing technology, 3D printing has gained increasing attention from scientists. This technology offers high design flexibility and the ability to produce complex components, reducing process complexity and enabling high production efficiency without material waste. Therefore, integrating 3D printing technology [36] into the fabrication of flexible PEDOT:PSS electrochromic devices shows promise for reducing overall process complexity, enabling bespoke production, and conserving materials [37].

In this work, we employ a concentration-controlled design strategy to develop a 3D-printable PEDOT:PSS conductive polymer ink with controllable rheological properties. The 3D-printed PEDOT:PSS films demonstrate excellent electrochromic performance, with an optical contrast of up to 47.9% at 635 nm, a high coloration efficiency of $352 \text{ cm}^2 \text{ C}^{-1}$, a fast coloration time of just 1.6 s, and an extremely short bleaching time of only 0.6 s. Notably, even after 100 electrochemical cycles, the optical contrast of the films decreases by only 9.3%, highlighting their outstanding cycling stability and durability. Finally, by leveraging the customization advantages of 3D printing, we fabricate flexible patterned electrochromic devices with bespoke butterfly designs using PEDOT:PSS conductive polymer ink. This work emphasizes the significant potential of 3D printing technology for practical applications such as flexible patterned displays and letter displays.

2 Materials and Methods

2.1 Materials

Poly(3,4-ethylenedioxythiophene):polystyrene sulfonate (PEDOT:PSS) (Orgacon DRY, Agfa Materials, Beijing, China), deionized water, lithium chloride (LiCl) were purchased from Aladdin, Shanghai, China. poly(vinyl alcohol) (PVA, Mw 146-186 kDa). ITO-PET ($<10 \Omega \text{ sq}^{-1}$) were purchased from Zhuhai Kaivo, Guangdong, China.

2.2 Preparation of Electrochromic Precursor Ink

First, 0.25 g of PEDOT:PSS particles (Orgacon DRY, Agfa Materials, Beijing, China) was added to 4.75 g of deionized water. The mixture was filtered several hundred times at room temperature using a syringe filter (40 μm) and then passed through a filter at least 15 times until fully homogenized. To ensure the ink was bubble-free, it was degassed using a centrifuge at 8000 rpm for 15 min. This process yielded a 3D-printable conductive polymer ink containing 5 wt% PEDOT:PSS. Additionally, the concentration of PEDOT:PSS particles was varied to prepare inks with 1, 3, and 7 wt% PEDOT:PSS conductive polymers.

2.3 PVALiCl Gel Electrolyte Preparation

First, 1 g of PVA and 1 g of LiCl were added to 8 g of deionized water. The solution was then stirred continuously at 90°C for two hours to ensure thorough mixing and dissolution. Once the solution cooled to room temperature and stabilized, it was ready to be cast onto the device.

2.4 3D-Printed Electrochromic Films

Flexible electrochromic films were produced using a direct ink writing 3D printer (DB 100, Shanghai MiFang Electronic Technology Co., Ltd., Shanghai, China) by optimizing 5 wt% PEDOT:PSS electrochromic inks. Needles of various sizes (90, 160, 210 and 240 μm) were employed during the printing process, with the air pressure adjusted between 0 and 500 kPa and the printing speed ranging from 2 to 20 mm/s. The 3D-printed layers were initially designed in Adobe Illustrator 2022 and saved in SVG format. Before printing, the SVG file was imported into the DB 100 software, where the model could be fine-tuned and printing parameters set before initiating the printing process.

2.5 Fabrication of Flexible Patterned ECDs

To improve the quality of the 3D-printed films, the conductive substrate needed to be pre-activated. The ITO-PET substrate was ultrasonically cleaned with acetone, ethanol, and deionized water for 10 min each, followed by a 5 min treatment with a UV ozone analyzer. The printed PEDOT:PSS film was dried and annealed at 60°C for 5 min. 3 M double-sided tape was then applied around the edges of the dried film, and the gel electrolyte was drop-cast onto it. Finally, another layer of ITO-PET was added to form a “sandwich” structure for the flexible electrochromic device (Fig. 1).

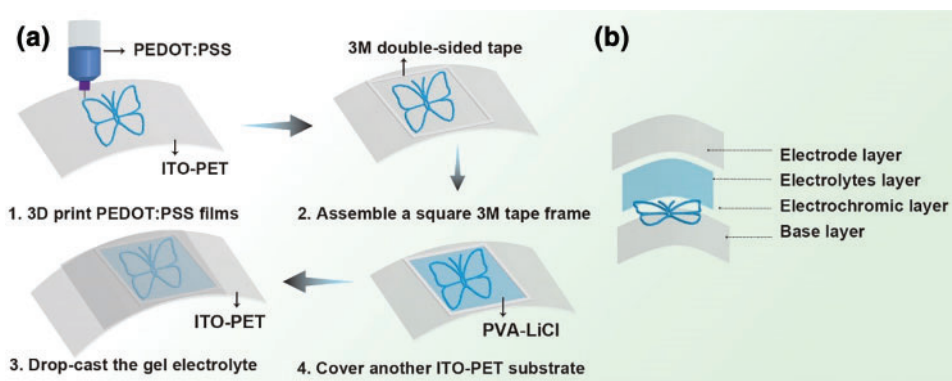


Figure 1: Integrated 3D printing of FECDs (a) Schematic diagram of the fabrication of a flexible electrochromic device. (b) Schematic diagram of a flexible electrochromic device structure

2.6 Electrochemical Properties

Electrochemical evaluations were performed using a Versa Stat 3 electrochemical workstation (EG&G Princeton Applied Research, Beijing, China). The redox behavior of the PEDOT:PSS film was examined through cyclic voltammetry using a conventional three-electrode setup, with glassy carbon as the working electrode, Ag/AgCl as the reference electrode, and Pt wire as the counter electrode. These analyses were conducted in an aqueous PVA-LiCl (0.1 M) solution under a nitrogen atmosphere, with various scan rates applied.

3 Result and Discussion

3.1 Device Design Strategy

The modern 3D printing technology has become quite mature, and integrating it into device fabrication processes offers numerous advantages [38,39]. The 3D printing technology used in this study allows for programmable and continuous printing of electrochromic materials with complex patterns, significantly reducing manual labor costs. Compared to screen printing and spin coating, this method also saves substantial amounts of raw materials, thereby reducing costs. This study introduces 3D printing technology to fabricate PEDOT-based conductive polymer electrochromic functional layers by designing different solid content PEDOT:PSS conductive polymer inks and optimizing the 3D printing parameters (Fig. 1a). The optimal printing parameters for 5 wt% PEDOT:PSS conductive polymer ink involve printing at a pressure of 100 kPa and a speed of 10 mm/s using a 160 μm nozzle. This allows precise printing of various patterns of PEDOT:PSS thin-film electrochromic functional layers on a flexible ITO-PET substrate. Additionally, the device structure is simplified, and the assembly process is optimized (Fig. 1b), providing theoretical guidance for subsequent 3D printing of PEDOT-based conductive polymers and the assembly of flexible electrochromic devices.

3.2 3D Printability Evaluation of Electrochromic Inks

To explore the 3D printability of the prepared PEDOT:PSS conductive polymer ink, the effects of different solid contents (1, 3, 5, 7, and 10 wt%) of PEDOT:PSS film on the viscoelasticity of the 3D-printable conductive polymer ink are investigated. Small amplitude shear oscillation experiments are conducted using strain sweep tests to eliminate ink overflow effects. As shown in Fig. 2a, the ink exhibits general characteristics of a viscous solution, with the storage modulus and loss modulus gradually increasing as the solid content of PEDOT:PSS increases from 1 to 10 wt%, and the storage modulus is higher than the loss modulus. This indicates that as the solid content increases, the elasticity of the ink is enhanced, leading to energy storage mainly in an elastic form rather than dissipation in other forms such as heat. Rheological behavior results show that the prepared 3D-printable PEDOT:PSS conductive polymer ink meets the characteristics of a polymer solution with pseudoplastic fluid behavior, specifically shear thinning (where the viscosity of the tested ink decreases as the shear rate increases), as shown in Fig. 2b. This occurs because the long, thin polymer chains align in the direction of flow to maintain a steady state as they move between layers of different flow velocities. This alignment becomes more pronounced as the shear rate increases, causing a reduction in solution viscosity. Additionally, as the solid content of PEDOT:PSS increases, the solution viscosity also gradually increases. The 3D-printed PEDOT:PSS electrochromic films exhibit excellent performance, and the microscopic morphology shows that the printed films are relatively uniform (Fig. A1).

3.3 Electrical and Optical Properties

Cyclic voltammetry of the PEDOT:PSS film is tested at different scan rates, ranging from 500 to 25 mV s^{-1} , in an electrolyte without a monomer. As shown in Fig. 2c, the results display broad anodic and cathodic peaks similar to those of PEDOT and its derivatives. The redox peak current density shows a good linear correlation with the potential scan rate, with a ratio close to 1 (Fig. 2d) [40,41], indicating that the PEDOT:PSS film has good adhesion to the modified electrode and exhibits reversible electrochemical activity and non-diffusion behavior.

The color change of the PEDOT:PSS films is directly tested in a three-electrode system using the PVA-LiCl gel electrolyte (0.1 mol L^{-1}). As shown in Fig. 2e, the PEDOT:PSS films exhibit a color transition from deep blue to light blue. The spectroelectrochemical curves of the PEDOT:PSS film is tested during the transition from its reduced state (-1 V) to its oxidized state (0.1 V), and the result is similar to those of other PEDOT:PSS electrochromic materials. The reduced (dedoped) PEDOT:PSS film exhibits a deep blue color with an absorption peak at 635 nm, attributed to the $\pi-\pi^*$ transition of the molecules. As the applied potential gradually shifts from a negative voltage (-1 V) to a positive voltage (0.1 V), the absorption peak at 635 nm decreases, indicating that with the increase in oxidation (doping), new polaron energy levels are formed between the valence and conduction bands, leading to the gradual formation of a new absorption peak at 948 nm. This peak is attributed to the π -polaron transition. The PEDOT:PSS film displays significant spectral and color changes throughout the redox process across the entire spectrum range (350 to 1100 nm). To more precisely identify the material's color, colorimetric measurements are conducted. The Commission Internationale de L'Eclairage (CIE) system is used as a quantitative scale to define and compare colors. As shown in Fig. 2f, during the redox conversion, the PEDOT:PSS film exhibits a deep blue color in its undoped (reduced) state (0.438, 0.395) and a light blue color in its fully doped (oxidized) state (0.371, 0.359).

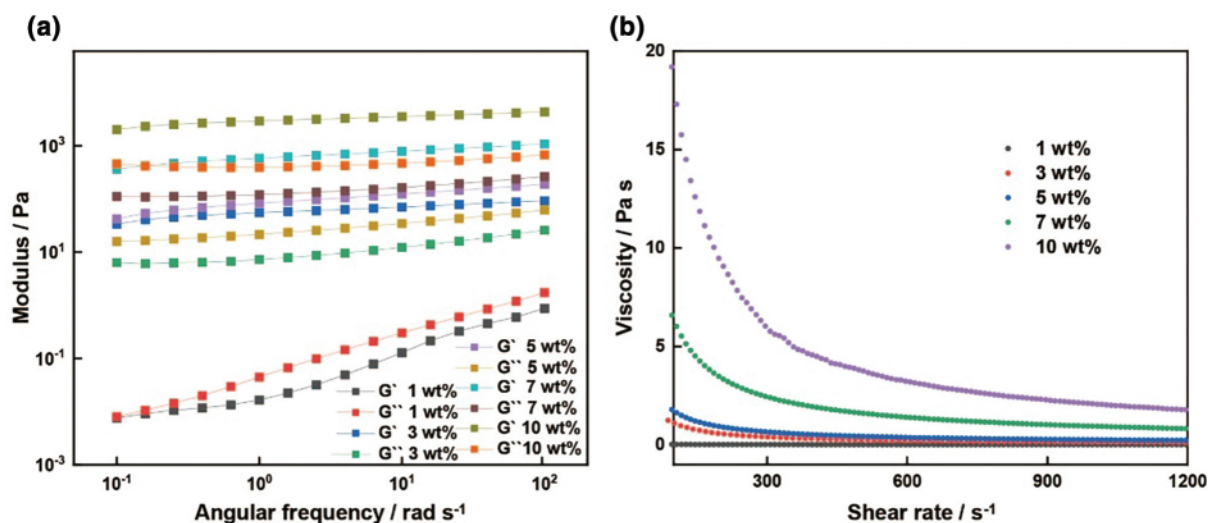


Figure 2: (Continued)

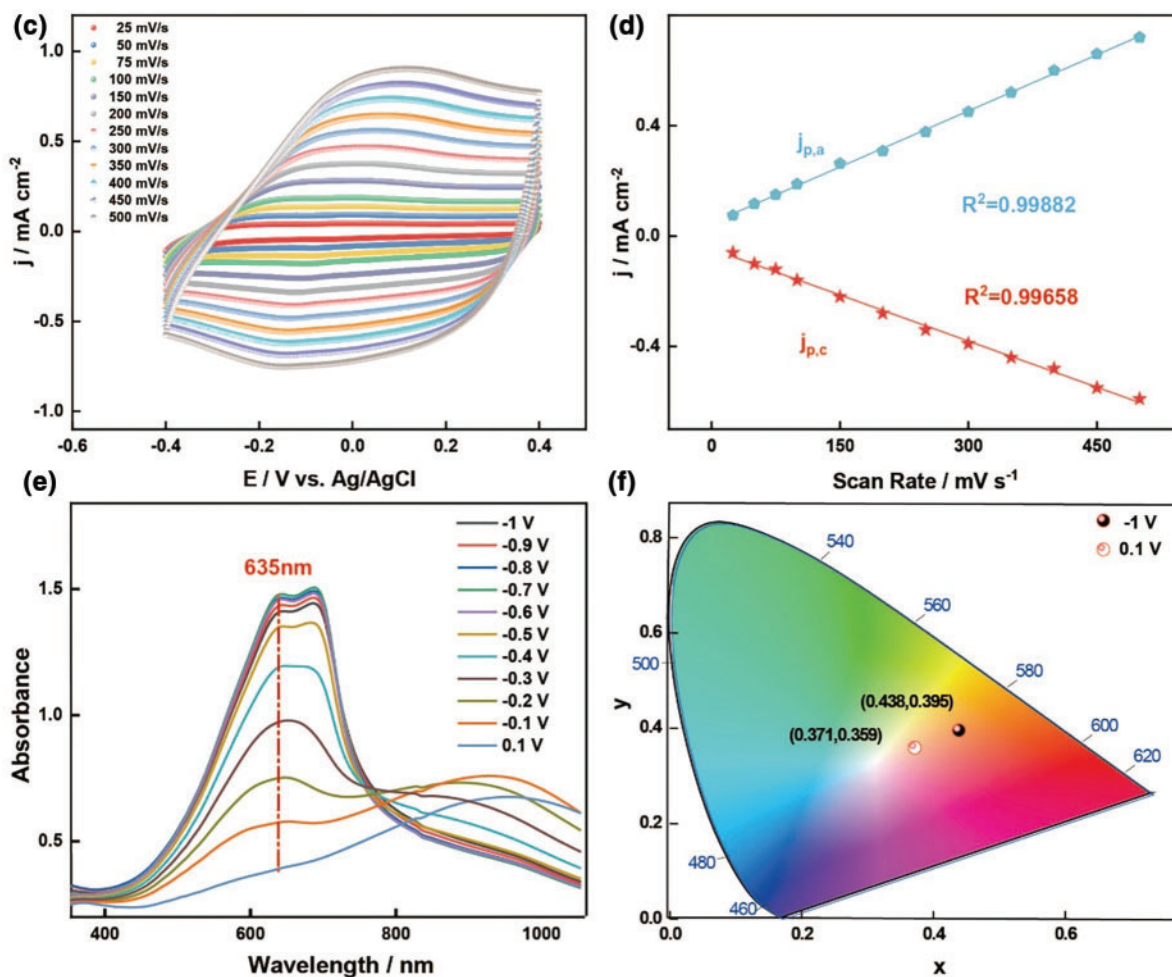


Figure 2: Evaluation of 3D printable electrochromic ink and the electrical and optical performance of electrochromic films. (a) Rheological properties of 3D printable conducting polymer inks about 1, 3, 5, 7 and 10 wt% PEDOT:PSS concentration. G' (open symbols) and G'' (closed symbols) as a function of shear strain. (b) Apparent viscosity as a function of shear rate for PEDOT:PSS conducting polymer inks of varying PEDOT:PSS concentration. (c) CVs of the PEDOT:PSS film-modified Pt electrode in PVA-LiCl at varying potential scan rates of 500, 450, 400, 350, 300, 250, 200, 150, 100, 75, 50, and 25 mV s^{-1} . (d) Corresponding linear dependence between scan rate and peak current density. $j_{p,a}$, anodic peak current density; $j_{p,c}$, cathodic peak current density. (e) Spectroelectrochemistry for PEDOT:PSS film on the ITO-glass in blank PVA-LiCl (0.1 mol L^{-1}). The applied potential was increased in 0.1 V increments from -1 to 0.1 V vs. Ag/AgCl. (f) CIE analysis of PEDOT:PSS film in the bleached and colored states

3.4 Electrochromic Properties of Integrated 3D Printed PEDOT:PSS FECDs

This work evaluates the effect of different solid contents PEDOT:PSS electrochromic films on the electrochromic performance, the optical contrast of 1, 3, 5, 7, and 10 wt% PEDOT:PSS electrochromic films are tested at 635 nm (Fig. A2). Among them, the 5 wt% PEDOT:PSS electrochromic films exhibit the highest optical contrast of 47.9%, while the other films achieve optical contrast of 33.7%, 29.5%, and 40.1%, respectively. The 5 wt% PEDOT:PSS electrochromic films demonstrate their coloring and bleaching times of 1.6 and 0.6 s at 635 nm (Fig. 3a). This electrochromic films exhibit excellent

coloration efficiency of $352 \text{ cm}^2 \text{ C}^{-1}$ (Fig. 3b). Stability is a crucial parameter for evaluating the practical application of PEDOT:PSS conductive polymers in flexible electrochromic devices. Long-term electrochemical testing of the PEDOT:PSS conductive polymer films is conducted under an applied voltage of -1 and 0.1 V at a wavelength of 635 nm (Fig. 3c). After 100 cycles of electrochemical testing, the optical contrast of the PEDOT:PSS film decreases by only 9.3% , maintaining excellent stability. After 1000 cycles, the optical contrast decreases by 46% . For electrochromic kinetics tests, parameters such as transmittance, response time, and stability are influenced not only by the applied voltage but also by the interval between voltage applications. The voltage range for electrochromic kinetics testing is -0.8 to 0.2 V . The transmittance-time curves of $5 \text{ wt}\%$ PEDOT:PSS electrochromic film are systematically studied at potential switching intervals of $20, 15, 10, 8, 5, 3,$ and 1 s (Fig. 3d). As the potential switching interval decreased, the optical contrast of the PEDOT:PSS film shows a decreasing trend. When the time interval decreased from 20 to 10 s , the optical contrast only decreased by 0.6% ; when the interval was reduced to 1 s , the optical contrast of the PEDOT:PSS electrochromic film decreased by 11.7% . In comparison with other PEDOT:PSS based electrochromic materials [42–46], the superior electrochromic performance of this work is demonstrated (Table A1, Fig. A3).

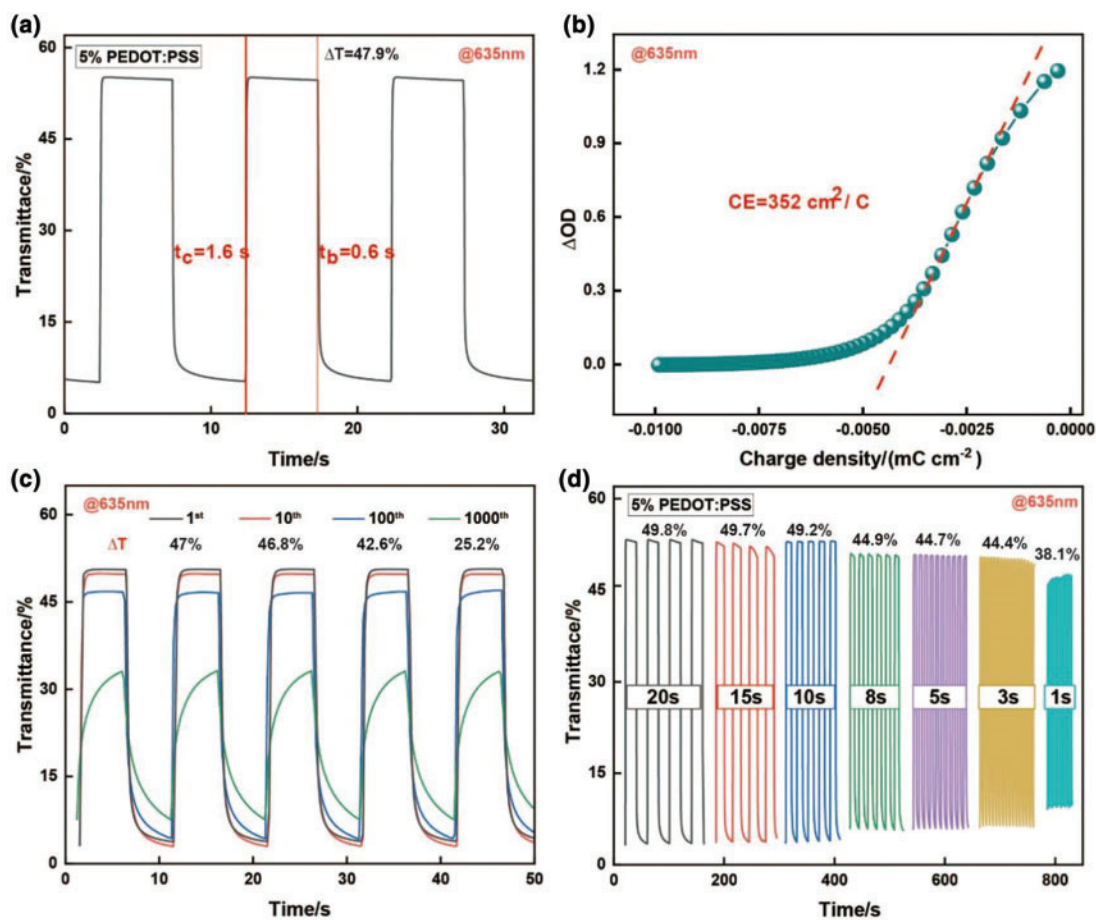


Figure 3: Evaluation of the electrochromic performance of PEDOT:PSS films. (a) Optical contrast and response time of a $5 \text{ wt}\%$ PEDOT:PSS film at 635 nm . (b) Coloration efficiency of a $5 \text{ wt}\%$ PEDOT:PSS film at 635 nm . (c) Long-term stability test of PEDOT:PSS films at 635 nm . (d) Optical contrast evaluation of a $5 \text{ wt}\%$ PEDOT:PSS film at different switching times ($20, 15, 10, 8, 5, 3,$ and 1 s) at 635 nm

3.5 Integrated 3D Printed FECDs for Patterned Displays

To better observe the electrochromic phenomenon, a large-area (4 cm × 4 cm) butterfly-patterned PEDOT:PSS electrochromic device is constructed. A flowchart is drawn to illustrate the continuous production process of the PEDOT:PSS conductive polymer electrochromic functional layer through 3D printing (Fig. 4a), and the reversible color transition of the rigid electrochromic device on an ITO-PET substrate in the voltage range of -1 to 0.1 V is demonstrated (Fig. 4b). The flexible PEDOT:PSS electrochromic device clearly exhibits a reversible color transition from deep blue to light blue under a voltage range of -1 to 0.1 V. At -1 V, a deep blue butterfly is displayed, and as the voltage increases, the color gradually fades until a light blue butterfly appears. The device's color-changing effect is unaffected by bending or folding. Fig. 4c shows that the device achieved the deep blue-to-light blue transition even when bent. These patterned applications highlight the multifunctionality of 3D-printed FECDs and demonstrate their potential for use in flexible display electronics.

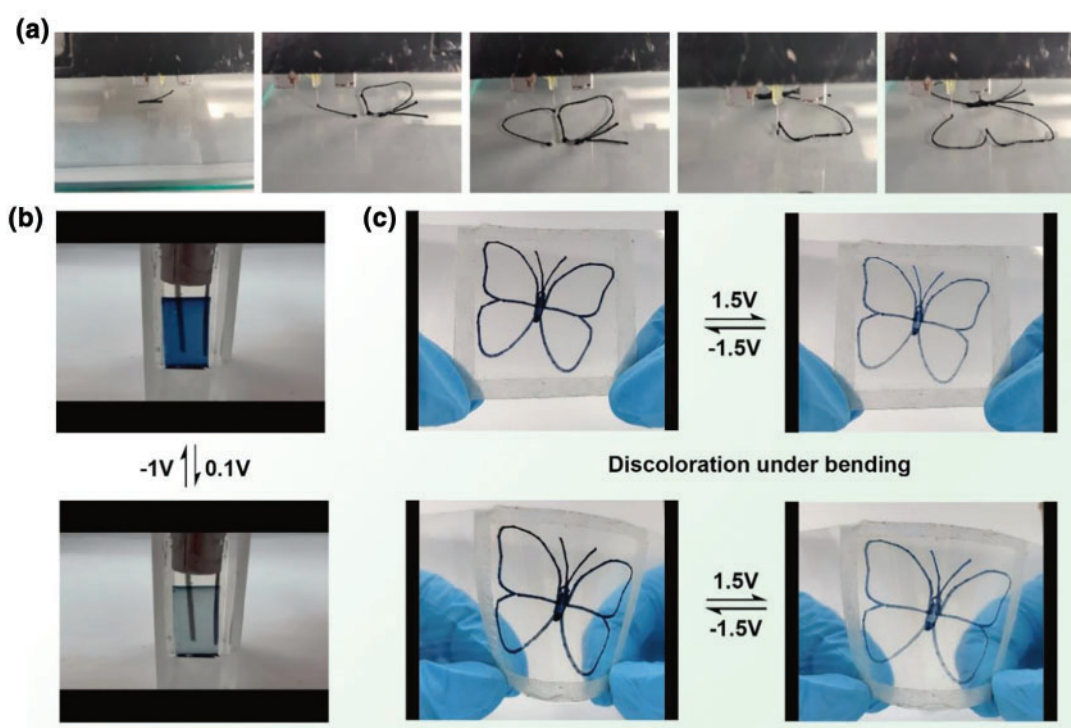


Figure 4: Process flow diagram for 3D printed electrochromic films, color change images, and patterned applications of flexible PEDOT:PSS electrochromic devices in the visible light region. (a) Process flow diagram for 3D printing a 5 wt% PEDOT:PSS butterfly-patterned electrochromic functional layer. (b) Reversible color change images of the 5 wt% PEDOT:PSS film under different voltages. (c) Images of the butterfly-patterned flexible electrochromic device that reversibly changes color under relaxed and bent conditions

4 Conclusion

This study employs a concentration control strategy to develop a 3D-printable ink with tailored rheological properties, enabling programmable patterning and the rapid fabrication of PEDOT-based conductive polymer electrochromic functional layers. The electrical and stability performances of

the prepared PEDOT:PSS films are evaluated, demonstrating excellent electrochromic properties. A flexible electrochromic device based on PEDOT:PSS conductive polymers is then constructed, highlighting its potential applications in flexible electronics, such as patterned and letter displays. This work provides theoretical insights and technical support for advancing the research and large-scale application of high-performance flexible electrochromic devices.

Acknowledgement: None.

Funding Statement: This work was financially supported by the Natural Science Foundation of Jiangxi Province (20232ACB204002 & 20232BAB202044) and Jiangxi Provincial Key Laboratory of Flexible Electronics (20212BCD42004 & 20242BCC32010).

Author Contributions: Manting Song: Writing—review & editing, Writing—original draft, Software, Formal analysis, Data curation, Experiment, Conceptualization. Changchen Gong: Writing—review & editing, Writing—original draft, Experiment, Formal analysis, Data curation. Ximei Liu: Writing—review & editing, Writing—original draft, Resources, Supervision, Data curation, Conceptualization, Funding acquisition. All authors reviewed the results and approved the final version of the manuscript.

Availability of Data and Materials: The datasets generated and/or analyzed during the current study are available from the corresponding author on reasonable request.

Ethics Approval: Not applicable.

Conflicts of Interest: The authors declare no conflicts of interest to report regarding the present study.

References

1. Rafsanjani A, Coulter FB, Studart AR. Giving life to robotic skins. *Matter*. 2022;5(7):1990–2. doi:10.1016/j.matt.2022.06.006.
2. Koo J, Amoli V, Kim SY, Lee C, Kim J, Park SM, et al. Low-power, deformable, dynamic multicolor electrochromic skin. *Nano Energy*. 2020;78:105199. doi:10.1016/j.nanoen.2020.105199.
3. Rogers JA. Wearable electronics nanomesh on-skin electronics. *Nat Nanotechnol*. 2017;12(9):839–40. doi:10.1038/nnano.2017.150.
4. Wu ZX, Zhao Q, Luo XY, Ma HD, Zheng WQ, Yu JW, et al. Low-cost fabrication of high-performance fluorinated polythiophene-based vis-NIR electrochromic devices toward deformable display and camouflage. *Chem Mater*. 2022;34(22):9923–33. doi:10.1021/acs.chemmater.2c01964.
5. Luo XY, Wan RT, Zhang ZX, Song MT, Yan LX, Xu JK, et al. 3D-Printed hydrogel-based flexible electrochromic device for wearable displays. *Adv Sci*. 2024;11(38):2404679. doi:10.1002/advs.202404679.
6. Wu SD, Sun HL, Duan MF, Mao HJ, Wu YF, Zhao HX, et al. Applications of thermochromic and electrochromic smart windows: materials to buildings. *Cell Rep Phys Sci*. 2023;4(5):101370.
7. Gupta J, Shaik H, Gupta VK, Sattar SA. Perspective of electrochromic double layer towards enrichment of electrochromism: a review. *Braz J Phys*. 2024;54(3):89.
8. Sun JW, Chen YN, Liang ZQ. Electroluminochromic materials and devices. *Adv Funct Mater*. 2016;26(17):2783–99.
9. Constantin CP, Damaceanu MD. A refreshing perspective on electrochromic materials: phenoxazine as an opportune moiety towards stable and efficient electrochromic polyimides. *Chem Eng J*. 2023;465:142883.
10. Gu C, Wang S, He JL, Zhang YM, Zhang SXA. High-durability organic electrochromic devices based on *in-situ*-photocurable electrochromic materials. *Chem*. 2023;9(10):2841–54.
11. Cihaner A, Algi F. A novel neutral state green polymeric electrochromic with superior n- and p-doping processes: closer to red-blue-green (RGB) display realization. *Adv Funct Mater*. 2008;18(22):3583–9.

12. Sun Y, Shi M, Zhu YN, Perepichka IF, Xing X, Liu YM, et al. Multicolored cathodically coloring electrochromism and electrofluorochromism in regioisomeric star-shaped carbazole dibenzofurans. *ACS Appl Mater Interfaces*. 2020;12(21):24156–64.
13. Nguyen TTA, Soram BS, Tran DT, Kim NH, Lee JH. Enhanced electrochromic capacity performances of hierarchical MnO₂-polyaniline/PEDOT:PSS/Ag@Ni nanowires cathode for flexible and rechargeable electrochromic Zn-Ion battery. *Chem Eng J*. 2023;452:139555.
14. Xu B, Chen JW, Li P, Ouyang YJ, Ma Y, Wang HL, et al. Transparent metal oxide interlayer enabling durable and fast-switching zinc anode-based electrochromic devices. *Nanoscale*. 2023;15(48):19629–37.
15. Rao TK, Zhou YL, Jiang J, Yang P, Liao WG. Low dimensional transition metal oxide towards advanced electrochromic devices. *Nano Energy*. 2022;100:107479.
16. Ma DY, Wang JM. Inorganic electrochromic materials based on tungsten oxide and nickel oxide nanostructures. *Sci China Chem*. 2017;60(1):54–62. doi:10.1007/s11426-016-0307-x.
17. Wang Z, Wang XY, Cong S, Chen J, Sun HZ, Chen ZG, et al. Towards full-colour tunability of inorganic electrochromic devices using ultracompact fabry-perot nanocavities. *Nat Commun*. 2020;11(1):302. doi:10.1038/s41467-019-14194-y.
18. Liu L, Zhang QQ, Du K, He ZB, Wang T, Yi Y, et al. An intelligent and portable power storage device able to visualize the energy status. *J Mater Chem A*. 2019;7(40):23028–37. doi:10.1039/C9TA07553D.
19. Österholm AM, Nhon L, Shen DE, Dejneka AM, Tomlinson AL, Reynolds JR. Conquering residual light absorption in the transmissive states of organic electrochromic materials. *Mater Horiz*. 2022;9(1):252–60. doi:10.1039/D1MH01136G.
20. Wang XK, Chen K, de Vasconcelos LS, He JZ, Shin YC, Mei JG, et al. Mechanical breathing in organic electrochromics. *Nat Commun*. 2020;11(1):211. doi:10.1038/s41467-019-14047-8.
21. Bessinger D, Muggli K, Beetz M, Auras F, Bein T. Fast-switching vis-IR electrochromic covalent organic frameworks. *Adv Sci*. 2021;143(19):7351–7. doi:10.1021/jacs.0c12392.
22. Lutkenhaus J. A radical advance for conducting polymers. *Science*. 2018;359(6382):1334–5. doi:10.1126/science.aat1298.
23. Kang SD, Snyder GJ. Charge-transport model for conducting polymers. *Nat Mater*. 2017;16(2):252–7. doi:10.1038/nmat4784.
24. Tropp J, Collins CP, Xie XR, Daso RE, Mehta AS, Patel SP, et al. Conducting polymer nanoparticles with intrinsic aqueous dispersibility for conductive hydrogels. *Adv Mater*. 2024;36(1):2306691. doi:10.1002/adma.202306691.
25. Yoon H, Ha H, Choi C, Yun T, Hwang B. Mini review on PEDOT:PSS as a conducting material in energy harvesting and storage devices applications. *J Polym Mater*. 2023;40(1–2):1–17. doi:10.32381/JPM.2023.40.1-2.1.
26. Lu BY, Yuk H, Lin ST, Jian NN, Qu K, Xu JK, et al. Pure PEDOT:PSS hydrogels. *Nat Commun*. 2019;10:1043.
27. Yu J, Tian F, Wang W, Wan R, Cao J, Chen C, et al. Design of highly conductive, intrinsically stretchable, and 3D printable PEDOT:PSS hydrogels via PSS-Chain engineering for bioelectronics. *Chem Mater*. 2023;35(15):5936–44.
28. Yu J, Wan R, Tian F, Cao J, Wang W, Liu Q, et al. 3D printing of robust high-performance conducting polymer hydrogel-based electrical bioadhesive interface for soft bioelectronics. *Small*. 2024;20(19):2308778.
29. Li G, Guo CF. PEDOT:PSS-based intrinsically soft and stretchable bioelectronics. *Soft Sci*. 2022;2(2):7.
30. Matsuhisa N, Niu SM, O'Neill SJK, Kang JH, Ochiai Y, Katsumata T, et al. High-frequency and intrinsically stretchable polymer diodes. *Nature*. 2021;600(7888):246–52.
31. Zhao Q, Wang JK, Ai XH, Duan YJ, Pan ZH, Xie SR, et al. Three-dimensional knotting of W₁₇O₄₇@PEDOT:PSS nanowires enables high-performance flexible cathode for dual-functional electrochromic and electrochemical device. *Infomat*. 2022;4(4):12298.
32. Shao ZW, Huang AB, Ming C, Bell J, Yu P, Sun YY, et al. All-solid-state proton-based tandem structures for fast-switching electrochromic devices. *Nat Electron*. 2022;5:45–52.
33. Yang GJ, Fan JP, Zhang K, Gu C, Li J, Kang K, et al. Electrochromic reflective displays based on *In situ* photo-crosslinked PEDOT:PSS patterns. *Adv Funct Mater*. 2024;34(17):2314983.

34. Zhang H, Sun FY, Cao G, Zhou DY, Zhang GF, Feng JY, et al. Bifunctional flexible electrochromic energy storage devices based on silver nanowire flexible transparent electrodes. *Int J Extreme Manuf.* 2023;5:015503.
35. Cai GF, Darmawan P, Cui MQ, Wang JX, Chen JW, Magdassi S, et al. Highly stable transparent conductive silver grid/PEDOT:PSS electrodes for integrated bifunctional flexible electrochromic supercapacitors. *Adv Energy Mater.* 2016;6(4):1501882.
36. Chen J, Virrueta C, Zhang SM, Mao CB, Wang JL. 4D printing: the spotlight for 3D printed smart materials. *Mater Today.* 2024;77:66–91.
37. Cheng XY, Peng SQ, Wu LX, Sun QF. 3D-printed stretchable sensor based on double network PHI/PEDOT:PSS hydrogel annealed with cosolvent of H₂O and DMSO. *Chem Eng J.* 2023;470:144058.
38. Li J, Cao J, Lu B, Gu G. 3D-printed PEDOT:PSS for soft robotics. *Nat Rev Mater.* 2023;8(9):604–22.
39. Wang F, Xue Y, Chen X, Zhang P, Shan L, Duan Q, et al. 3D printed implantable hydrogel bioelectronics for electrophysiological monitoring and electrical modulation. *Adv Funct Mater.* 2024;34(21):2314471.
40. Wu W, Lee PS. Flexible and stretchable electrochromic displays: strategies, recent advances, and prospects. *Soft Sci.* 2024;4(3):29.
41. Du CH, Xu YH, Li H, Wu ZX, Yang HJ, Liu XM, et al. Tough hydrogen bonding crosslinked poly (3-fluorothiophene) network via electrosynthesis for high-performance electrochromic supercapacitors. *Chin J Polym Sci.* 2024;42:1749–57.
42. Yu H, Fang H, Jing K, Ma H, Wu L, Chai Y. Electrochromic devices based on 2D MoO_{3,x}/PEDOT:PSS composite film with boosted ion transport. *ACS Appl Mater Interfaces.* 2024;16(14):18052–62.
43. Li H, Zhang W, Elezzabi AY. Transparent zinc-mesh electrodes for solar-charging electrochromic windows. *Adv Mater.* 2020;32(43):2003574.
44. Yan S, Fu H, Zhang L, Dong Y, Li W, Ouyang M, et al. Conjugated polymer multilayer by *in situ* electrochemical polymerization for black-to-transmissive electrochromism. *Chem Eng J.* 2021;406:126819.
45. Ling H, Wu J, Su F, Tian Y, Liu YJ. Automatic light-adjusting electrochromic device powered by perovskite solar cell. *Nat Commun.* 2021;12:1010.
46. Cai G, Cui P, Shi W, Morris S, Lou SN, Chen J, et al. One-dimensional π -d conjugated coordination polymer for electrochromic energy storage device with exceptionally high performance. *Adv Sci.* 2020;7(20):1903109. doi:10.1002/advs.201903109.

Appendix A.

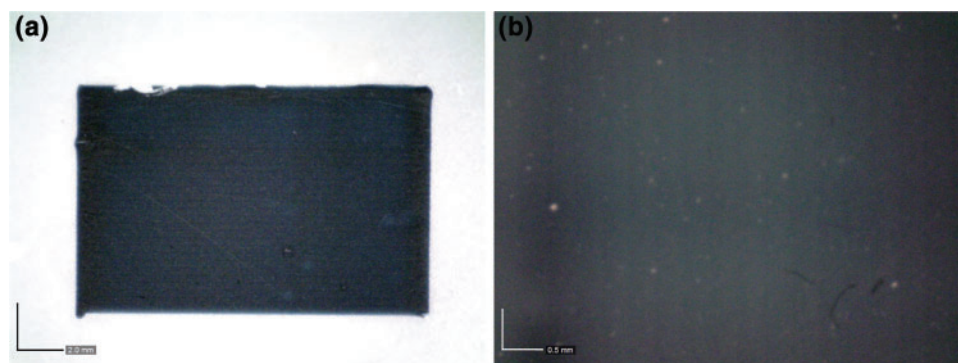


Figure A1: Microscopic images of PEDOT:PSS films. (a) Microscopic image at 2 mm scale. (b) Microscopic image at 0.5 mm scale

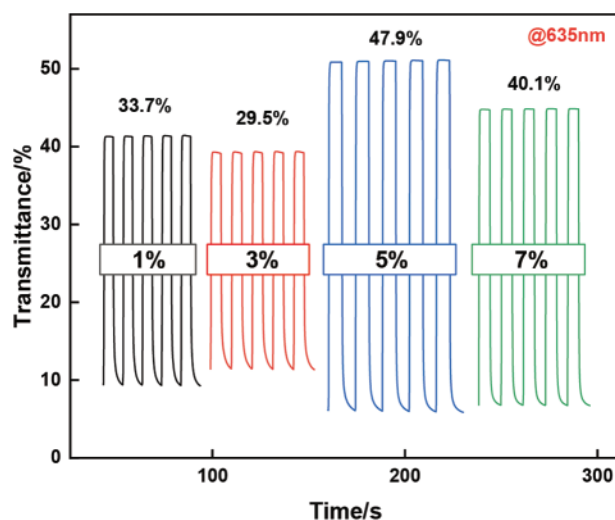


Figure A2: Optical contrast of PEDOT:PSS electrochromic materials with different solid content

Table A1: Comparison of electrochromic performance of different PEDOT:PSS-based electrochromic materials

Electrochromic materials	ΔT (%)	Response time (s) t_c / t_b	CE (cm^2 / C)	Stability	Ref
PEDOT:PSS	47.9	1.6/0.6	352	53.6%	This work
	635 nm			1000th	
MoO_{3-x} /PEDOT:PSS	65	7/5	87	91%	[42]
	670 nm			500th	
PEDOT:PSS/PMMA-TBAPF ₆	22	1/1	325	90%	[43]
	644 nm			500th	
PEDOT:PSS (Gelatin electrolyte)	36	1.6/1.4	105	47%	[44]
	685 nm			1000th	
PEDOT:PSS (PMMA-LiClO ₄)	62	3.2/5.7	135.1	85%	[45]
	700 nm			60th	
WO ₃ -PEDOT:PSS/H ₂ SO ₄	73.3	12.7/15.8	108.9	76.7%	[46]
	633 nm			200th	

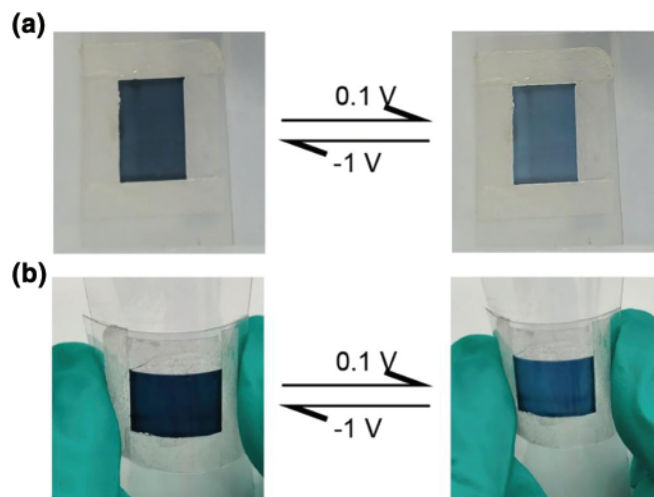


Figure A3: Images of the flexible electrochromic film that reversibly changes color. (a) The reversible color change of thin-film electrochromic devices in a relaxed state under voltage stimulation ranging from -1 to 0.1 V. (b) The reversible color change of thin-film electrochromic devices in a bent state under voltage stimulation ranging from -1 to 0.1 V